January 1, 2005

Asymptotic Analysis of Liquid Films Dip-Coated onto Chemically Micropatterned Surfaces

JM Davis

Jeffrey M. Davis

Asymptotic analysis of liquid films dip-coated onto chemically micropatterned surfaces

Jeffrey M. Davis[a)]
Department of Chemical Engineering, University of Massachusetts, Amherst, Massachusetts 01003

The dip coating of chemically heterogeneous surfaces is a useful technique for attaining selective material deposition. For the case of vertical, wetting stripes surrounded by nonwetting regions, experiments have demonstrated that the thickness of the entrained film on the stripes is significantly different than on homogeneous surfaces because of the lateral confinement of the liquid. In the present work, the asymptotic matching of equations based on lubrication theory is used to determine the film thickness, and necessary restrictions on the capillary and Bond numbers are provided. The predictions are in excellent agreement with the existing experimental data, and the classical Landau–Levich formula for homogeneous surfaces is recovered from the analysis in the limit of very wide stripes. © *2005 American Institute of Physics.* [DOI: 10.1063/1.1850751]

The dip coating of chemically homogeneous plates, rods, and fibers has been extensively investigated both experimentally and theoretically.[1–9] More recently, as microfabrication has become common and microfluidic applications have increased, the dip coating technique has been used to achieve selective material deposition on micropatterned surfaces.[10–13] In particular, the experimental investigation of the dip coating of vertical, wetting stripes on a nonwetting planar surface by Darhuber *et al.*[12] has demonstrated that fluid confinement by chemical surface patterning strongly affects the thickness of the entrained liquid film. For the general restrictions of small capillary and Bond numbers, scaling arguments were used to predict that the entrained film thickness at the center of the stripe, h_∞, scales as $h_\infty = b\widetilde{W}\text{Ca}^{1/3}$, where $\widetilde{W}$ is the width of the stripe and Ca is the capillary number defined below. The numerical prefactor b was not determined. Aside from the scaling arguments used by those authors, theoretical treatments have been confined to homogeneous surfaces for which the key step in the analysis, which has been presented with varying formality and rigor, entails the (one-dimensional) matching of the limiting curvature of the entrained liquid to that of a static meniscus of liquid on the substrate near the liquid reservoir. For the withdrawal of a homogeneous plate, the classical Landau–Levich result is[1]

$$h_\infty = 0.946 L_c \text{Ca}^{2/3}, \tag{1}$$

where L_c is the capillary length defined below. The scaling behavior observed by Darhuber *et al.* is clearly quite different, as the capillary length L_c is replaced by the much smaller stripe width $\widetilde{W}$, and the exponent of the capillary number decreases from 2/3 to 1/3. The dip coating of such micropatterned surfaces is reconsidered below, and asymptotic matching is used to determine the prefactor b. A simplified exposition is used in place of full mathematical rigor for brevity.

Consider the dip coating of a wetting microstripe of width $\widetilde{W}$ on a nonwetting plate that is withdrawn at velocity U from a bath containing liquid of density ρ, viscosity μ, and surface tension γ. The stripe is oriented vertically with the plate withdrawn in the $-x$ direction, as shown in Fig. 1, and z is directed outwardly normal from the plate surface. The component of the liquid velocity in the x direction is u, and it is assumed that the entrained liquid is completely confined to the wetting strip. (Such confinement was attained experimentally by Darhuber *et al.*[12])

Far above the reservoir, as $x \to -\infty$, the thickness of the entrained liquid film is independent of x and has centerline thickness $h|_{y=0} \equiv h_o = h_\infty$. In this region only viscous forces (and possibly gravity) determine the upward flux of liquid. At the reservoir the free surface profile (Fig. 2) is a static meniscus whose shape is governed by the balance of capillary and possibly hydrostatic pressures. The lubrication film transitions to the static meniscus through the dynamic meniscus, or overlap region, in which the viscous and capillary forces balance. The film curvature in this region smoothly matches the static meniscus curvature at the lower end, and the centerline film thickness decays to h_∞ as the lubrication film is approached for $x \to -\infty$.

The flow is described by the equations of lubrication theory, which are

$$-\frac{\partial p}{\partial x} + \rho g + \mu \frac{\partial^2 u}{\partial z^2} = 0 \tag{2}$$

and

$$-p = \gamma\kappa = -\gamma\boldsymbol{\nabla}_s \cdot \mathbf{n} \approx \gamma(h_{xx} + h_{yy}), \tag{3}$$

where p is the capillary pressure, κ is the (mean) curvature of the free surface at $y = h$, $\mathbf{n}$ is the unit normal vector directed outward from the liquid surface, $\boldsymbol{\nabla}_s$ is the surface gradient operator, and h is the film thickness. This analysis is restricted to small capillary numbers, $\text{Ca} = \mu U/\gamma \ll 1$, so that the viscous contributions to the normal stress balance at the free surface,[14] which would enter at $O(\text{Ca}^{2/3})$, may be ne-
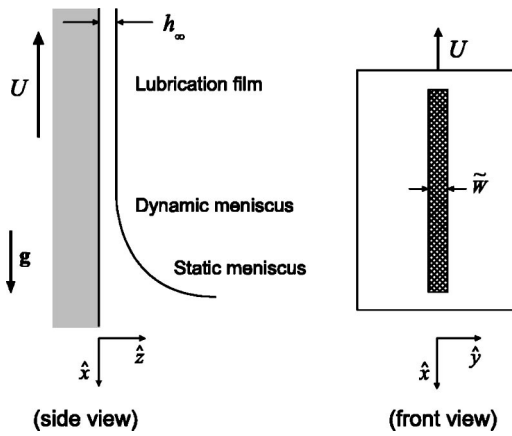
FIG. 1. Sketch of the dip coating geometry for the chemically micropatterned surface. The image at left is a side view of the film profile. The wetting microstripe of width $\widetilde{W}$ is indicated by the cross hatching in the image at right. The plate surface surrounding the microstripe is nonwetting.

glected in Eq. (3). These equations are solved subject to the boundary conditions of no slip at the solid-liquid interface,

$$u = -U \quad \text{at} \quad z = 0, \tag{4}$$

and vanishing shear stress at the liquid-air interface,

$$\mu \frac{\partial u}{\partial z} = 0 \quad \text{at} \quad z = h(x,y). \tag{5}$$

The velocity u is found by integrating Eq. (2) and using the boundary conditions given in Eqs. (4) and (5). A further integration with respect to z yields the flux Q, which is set equal to its asymptotic value as $x \to -\infty$ to give

$$h^3 \frac{\partial \kappa}{\partial x} = 3\text{Ca}(h - \widetilde{h}_\infty) + \frac{\rho g}{\gamma}(\widetilde{h}_\infty^3 - h^3), \tag{6}$$

where subscripts denote differentiation and $h \to \widetilde{h}_\infty$ as $x \to -\infty$. In addition to the geometric length scale $W \equiv \widetilde{W}/\sqrt{8}$, there are two natural length scales based on fluid properties: $d = (\mu U/\rho g)^{1/2}$, an apparent scale of the film
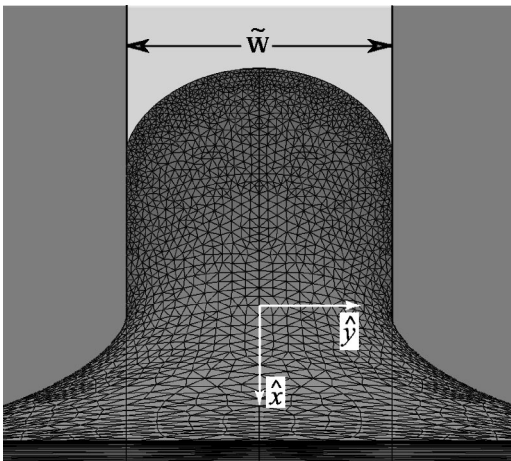

FIG. 2. Sketch of the free-surface profile of the static meniscus. The light gray region of width $\widetilde{W}$ is the wetting microstripe, and the surrounding dark gray region is nonwetting.

thickness, and $L_c = (\gamma/\rho g)^{1/2}$, which is the scale of a hydrostatic meniscus. Introducing the variables $H = h/d$, $X = x/L_c$, and $Y = y/W$ into Eq. (10) and substituting $\kappa \approx h_{xx} + h_{yy}$ yields

$$H^3[H_{XXX} + \text{Bo}^{-1}H_{YYX}] = 3\delta^{-3}(H - H_\infty) + \delta^{-3}(H_\infty^3 - H^3), \tag{7}$$

where $\delta^2 \equiv (d/L_c)^{2/3} = \text{Ca}^{1/3}$ is small and $\text{Bo} \equiv (W/L_c)^2 = \rho g W^2/\gamma$ is the Bond number.

If $\text{Bo} \gg 1$, then the stripe width is much larger than the capillary length, and the flat-plate solution should be a reasonable first approximation. The $H^3 H_{XXX}$ term will balance the viscous terms on the right-hand side if the new variables $\chi = \delta^{-2}X$ and $\psi = \delta^{-1}H$ are used to transform Eq. (7) into

$$\psi^3 \psi_{\chi\chi\chi} + \text{Bo}^{-1}\delta^4 \psi^3 \psi_{YY\chi} = 3(\psi - \psi_\infty) + \delta^2(\psi_\infty^3 - \psi^3). \tag{8}$$

These scales are identical to those used in analyses of the dip coating of a homogeneous flat plate[5] and a cylindrical rod of radius $R \gg L_c$.[15]

Substituting $\psi = h_\infty \phi$ and $\chi = 3^{-1/3}h_\infty \zeta$ and neglecting the small terms ($\text{Bo}^{-1} \ll 1$, $\delta^2 \ll 1$) due to the change in transverse curvature and drainage due to gravity converts Eq. (8) (to leading order) to the universal form

$$\phi^3 \phi_{\zeta\zeta\zeta} = \phi - 1, \tag{9}$$

subject to the boundary condition $\phi \to 1$ as $\zeta \to -\infty$. As $\zeta \to \infty$, $\phi_{\zeta\zeta} \to a$, which is a constant that can be found by integrating Eq. (9) numerically. Equating this constant, limiting curvature of the lubrication film region with the limiting curvature of the hydrostatic meniscus in a common set of scaled variables completes the matching process in the overlap region and leads to Eq. (1). The formal matching of rigorous asymptotic expansions in the thin film and meniscus regions has been presented up to $O(\delta^2)$ by Wilson.[5] The related problem of films climbing a homogeneous plane wall under the influence of surface tension gradients has also been studied.[16,17]

Now consider the case $\text{Bo} \ll 1$, which is the relevant limit for the dip coating of chemically patterned surfaces with arrays of vertical wetting microstripes. Because of the restriction $\text{Ca} \ll 1$, an $x = \text{const}$ cross section of the free surface of the liquid along the microstripe must be an arc of a circle,[18] which, within the lubrication approximation, simplifies to a parabola. The substitution $h(x,y) = h_o(x)[1 - 4(y/\widetilde{W})^2]$ then reduces the analysis to a one-dimensional matching problem to determine h_o, the film thickness along the centerline of the stripe, which is governed by

$$h_o^3(h_{oxxx} - W^{-2}h_{ox}) = 3\text{Ca}(h_o - h_\infty) + \frac{\rho g}{\gamma}(h_\infty^3 - h_o^3). \tag{10}$$

For these narrow stripes the transverse curvature of the liquid ribbon is significant, and Eq. (10) must be scaled such that both curvature terms are comparable to the viscous terms. Introducing the new variables $\xi = x/W$ and $\eta = h_o/[W(3\text{Ca})^{1/3}]$ transforms Eq. (10) into

$$\eta^3(\eta_{\xi\xi\xi} - \eta_\xi) = \eta - \eta_\infty + \text{Bo}(3\text{Ca})^{-1/3}(\eta_\infty^3 - \eta^3). \tag{11}$$

Neglecting the effects of drainage by gravity, which correspond to the last term in Eq. (11), therefore requires

$Bo(3Ca)^{-1/3} \ll 1$, which is more stringent than the constraint $\rho g h_\infty^2 / \gamma \ll 1$ (equivalent to $BoCa^{2/3} \ll 1$) given by Darhuber *et al.*[12]

At leading order, the free surface shape is therefore governed by

$$\eta^3(\eta_{\xi\xi\xi} - \eta_\xi) = \eta - \eta_\infty, \qquad (12)$$

subject to the boundary condition $\eta \to \eta_\infty$ as $\xi \to -\infty$. As $\xi \to \infty$, $\eta_{\xi\xi} - \eta \to C_S$, which is a constant that can be found by numerically integrating Eq. (12). The entrained film thickness is thus given by $h_\infty = \eta_\infty W (3Ca)^{1/3}$, where the numerical value of the constant η_∞ must be determined such that C_S is equal to the limiting curvature of the meniscus when expressed in a common set of variables.

In the meniscus region, W is the appropriate scale for x, y, and h, which is analogous to the use of the cylinder radius to scale both coordinates in the inner region for the static meniscus on a thin cylinder.[19] Introducing the new variables $\widetilde{H} = h/W$, $\widetilde{X} = x/W$, and $\widetilde{Y} = y/W$ into Eq. (6) yields

$$\widetilde{H}^3 \frac{\partial \widetilde{\kappa}}{\partial \widetilde{X}} = 3Ca(\widetilde{H} - \widetilde{H}_\infty) + Bo(\widetilde{H}_\infty^3 - \widetilde{H}^3), \qquad (13)$$

where $\widetilde{\kappa} = W\kappa$. The shape of the meniscus is therefore not influenced by the motion of the plate or by gravity at the level of approximation made earlier. As noted in an analytical study of the shape of the (static) liquid meniscus near a stripwise heterogeneous wall,[20] for $Bo \ll 1$ the interface within several stripe widths from the wall is a minimal surface with zero mean curvature ($\kappa = 0$). Because of the constraint $Bo \ll (3Ca)^{1/3}$ required to neglect gravity in Eq. (11), terms of $O(Bo)$ are uniformly negligible, and corrections to the shape of the meniscus due to inclusion of gravity are insignificant. In order to match the thin film and meniscus solutions in the overlap region, the constraint $\kappa = 0$, corresponding to the equality of the two principal radii of curvature, is therefore sufficient for negligible Bond number as only the limiting value of the mean curvature of the free surface at the top of the meniscus is needed. (If corrections for small but finite Bond number are desired, the exact meniscus profile must be determined numerically.) Evaluating κ along the centerline $y = 0$ and noting that the free surface must be symmetric (and that $h_x \to 0$ at the top of the meniscus to match the lubrication film) reveals that $\widetilde{H}_{\widetilde{X}\widetilde{X}} + \widetilde{H}_{\widetilde{Y}\widetilde{Y}} \to C_M = 0$ is the desired limiting behavior at the top of the meniscus to which the solution in the microstripe should be matched.

A standard shooting method can be used to determine the appropriate value of the constant η_∞. Linearizing about $\eta = \eta_\infty$, which is valid for $\xi \to -\infty$, provides the initial conditions required to integrate Eq. (12) numerically. The matching condition that $C_S = C_M$ requires that $\eta_{\xi\xi} - \eta \to 0$ as $\xi \to \infty$, which occurs for $\eta_\infty = 0.699\,11$. The final result for the thickness of the entrained liquid ribbon is then

$$h_\infty = \eta_\infty W (3Ca)^{1/3} = 0.24717 \widetilde{W}(3Ca)^{1/3}. \qquad (14)$$

This matching procedure can be extended to include corrections for small values of the Bond number (i.e., $Ca \ll Bo \ll Ca^{1/3}$) and generalized to the $Bo = O(1)$ regime for
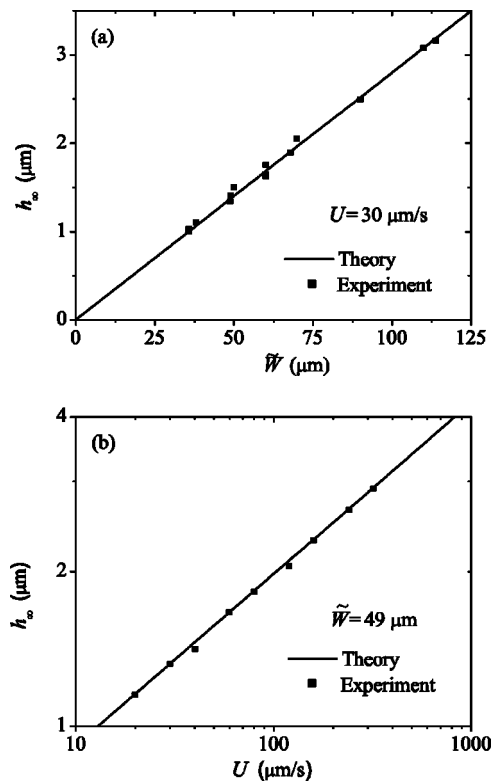

FIG. 3. Comparison of the prediction of Eq. (14) to the experimental data of Darhuber *et al.* (Ref. 12) for entrained film thickness h_∞ vs (a) stripe width $\widetilde{W}$ and (b) withdrawal velocity U for 4 mm long stripes from a bath of glycerol. In (a), $U = 30$ μm/s. In (b), $\widetilde{W} = 49$ μm. The symbols represent the experimental data, while the line is the theoretical prediction.

which the effects of both gravity and the transverse curvature of the liquid profile must be taken into account. Because W influences the shape of the static meniscus and the dynamics of the liquid in the overlap region, a general scaling law cannot be found, but the thickness of the entrained liquid film transitions from Eq. (14) to Eq. (1) as the stripe width increases. As indicated in Eq. (13), the (static) meniscus shape is determined by the balance of Laplace and hydrostatic pressure, and the limiting curvature $\widetilde{C}_M$ at the top of the meniscus can be calculated numerically. The entrained film thickness is then specified by asymptotically matching the curvature in the dynamic meniscus to $\widetilde{C}_M$ for given values of Bo and Ca.

For microstripes ranging from 40 to 110 μm, Darhuber *et al.* reported experimental results for the entrained film thickness as a function of the stripe width and the velocity with which the micropatterned plate was withdrawn from a bath of glycerol.[12] The experimental data are plotted with the predictions of Eq. (14) in Fig. 3. Extremely good agreement between the theoretical predictions and experimental results is attained. For the 23 published experimental measurements, $h_\infty / [(3Ca)^{1/3}\widetilde{W}] = 0.247 \pm 0.010$, which is in exact agreement with the theoretical prediction of Eq. (14). The experiments encompassed the ranges $2.5 \times 10^{-4} \leq Bo \leq 2.6 \times 10^{-3}$ and $3.1 \times 10^{-4} \leq Ca \leq 4.9 \times 10^{-3}$, with $Bo(3Ca)^{-1/3} \leq 0.023$, for which Eq. (14) is expected to be extremely accurate.

The dip coating of a thin, cylindrical fiber is similar to

that of a microstripe in that the fiber radius is a geometrically imposed length scale that enters the result for the film thickness because the curvature induced by the fiber radius is important in the meniscus region. In the thin film region, however, the term corresponding to the pressure induced by the curvature of the free surface in the direction transverse to flow is a constant until $O(\delta^4)$.[15] To the first orders of approximation its derivative is zero, and there is no resulting dynamical effect. With an appropriate change of variables, the governing equation for a cylinder in the overlap region thus reduces to the universal form given in Eq. (9) for a flat plate. The matching of $\lim_{\zeta \to \infty} \phi_{\zeta\zeta}$ to the streamwise curvature of the meniscus proceeds as for the flat plate, and the same $Ca^{2/3}$ dependence results. The only difference is that the streamwise curvature of the meniscus is controlled by the transverse curvature due to the cylindrical geometry (and not by the capillary length). For a microstripe, by contrast, the transverse curvature is important throughout the film, as the streamwise change in the transverse curvature, as represented by the $W^{-2} h_{ox}$ term in Eq. (10), balances the change in streamwise curvature (h_{oxxx}). Unlike the withdrawal of a cylinder, h_{oxx} does not approach a constant as $x \to \infty$. Instead, the total curvature (represented by $h_{oxx} - W^{-2} h_{ox}$) matches the full curvature of the meniscus. The importance of the change in transverse curvature with distance from the meniscus results in the novel $Ca^{1/3}$ dependence of the entrained film thickness.

Finally, in the equivalent limit of negligible gravity for the withdrawal of a cylinder ($Bo \equiv \rho g R^2 / \gamma \ll 1$), the requirement of zero mean curvature is analogously sufficient to determine h_∞, and the matching condition is that the streamwise curvature in the overlap region asymptotes to the inverse of the fiber radius. Because of the assumption $Bo \gg Ca$ made in the analysis of Wilson[15] (in contrast to the requirement $Bo \ll Ca^{1/3}$ in the present analysis), modifications of the meniscus shape due to gravity are considered, and a numerical solution for the (nonzero) meniscus curvature is needed.

[1] L. D. Landau and B. V. G. Levich, "Dragging of a liquid by a moving plate," Acta Physicochim. URSS **17**, 42 (1942).
[2] B. M. Deryagin and S. M. Levi, *Film Coating Theory* (Focal, New York, 1964).
[3] D. A. White and J. A. Tallmadge, "Theory of drag out of liquids on flat plates," Chem. Eng. Sci. **20**, 33 (1965).
[4] C. Y. Lee and J. A. Tallmadge, "Description of meniscus profiles in free coating," AIChE J. **18**, 858 (1972).
[5] S. D. R. Wilson, "The drag-out problem in film coating theory," J. Eng. Math. **16**, 209 (1982).
[6] O. Reglat, R. Labrie, and P. A. Tanguy, "A new free-surface model for the dip coating process," J. Comput. Phys. **109**, 238 (1993).
[7] P. R. Schunk, A. J. Hurd, and C. J. Brinker, in *Liquid Film Coating*, edited by S. F. Kistler and P. M. Schweizer (Chapman and Hall, London, 1997).
[8] D. Quéré, "Fluid coating on a fiber," Annu. Rev. Fluid Mech. **31**, 347 (1999).
[9] S. J. Weinstein and K. J. Ruschak, "Coating flows," Annu. Rev. Fluid Mech. **36**, 29 (2004).
[10] D. Qin, Y. Xia, B. Xu, H. Yang, C. Zhu, and G. M. Whitesides, "Fabrication of ordered two-dimensional arrays of micro- and nanoparticles using patterned self-assembled monolayers as templates," Adv. Mater. (Weinheim, Ger.) **11**, 1433 (1999).
[11] H. G. Braun and E. Meyer, "Thin microstructured polymer films by surface-directed film formation," Thin Solid Films **345**, 222 (1999).
[12] A. A. Darhuber, S. M. Troian, J. M. Davis, S. M. Miller, and S. Wagner, "Selective dip-coating of chemically micropatterned surfaces," J. Appl. Phys. **88**, 5119 (2000).
[13] H. Y. Fan, Y. F. Lu, A. Stump, S. T. Reed, T. Baer, R. Schunk, V. Perez-Luna, G. P. Lopez, and C. J. Brinker, "Rapid prototyping of patterned functional nanostructures," Nature (London) **405**, 56 (2000).
[14] R. P. Spiers, C. V. Subbaraman, and W. L. Wilkinson, "Free coating of a newtonian liquid onto a vertical surface," Chem. Eng. Sci. **29**, 389 (1974).
[15] S. D. R. Wilson, "Coating flow on to rods and wires," AIChE J. **34**, 1732 (1988).
[16] P. Carles and A.-M. Cazabat, "The thickness of surface-tension-gradient-driven spreading films," J. Colloid Interface Sci. **157**, 196 (1993).
[17] X. Fanton, A. M. Cazabat, and D. Quéré, "Thickness and shape of films driven by a Marangoni flow," Langmuir **12**, 5875 (1996).
[18] L. A. Romero and F. G. Yost, "Flow in an open channel capillary," J. Fluid Mech. **322**, 109 (1996).
[19] L. L. Lo, "The meniscus on a needle—a lesson in matching," J. Fluid Mech. **132**, 65 (1983).
[20] L. Boruvka and A. W. Neumann, "An analytical solution of the Laplace equation for the shape of liquid surfaces near a stripwise heterogeneous wall," J. Colloid Interface Sci. **65**, 315 (1978).